Food Chemistry: X 21 (2024) 101069

Contents lists available at ScienceDirect

Food Chemistry: X

journal homepage: www.sciencedirect.com/journal/food-chemistry-x

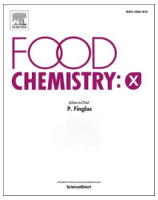

Development of fluorescent GO-AgNPs-Eu^{3+} nanoparticles based paper visual sensor for foodborne spores detection

Jiaqi Tian [a,b], Qiancheng Tu [a,b], Miaoyun Li [a,b], Lijun Zhao [a,b], Yaodi Zhu [a,b,c,*], Jong-Hoon Lee [d], Zhengyan Gai [c], Gaiming Zhao [a,b], Yangyang Ma [a,b]

[a] College of Food Science and Technology, Henan Agricultural University, Zhengzhou 450002, PR China
[b] International Joint Laboratory of Meat Processing and Safety in Henan Province, Henan Agricultural University, Zhengzhou 450002, PR China
[c] Henan Jiuyuquan Food Co., LTD. Postdoctoral Innovation Base, Henan Province, Yuanyang 453500, PR China
[d] Kyonggi University, Yongin-si 32588, Korea

ARTICLE INFO

Keywords:
Food-borne spores
2,6-Dipicolinic acid
Paper sensor
GO-AgNPs-Eu^{3+}
Fluorimetric sensing
Visualization

ABSTRACT

Foodborne spores are ubiquitous with extremely strong resistance, and pose a serious threat to food safety and human health. Therefore, rapid, sensitive, and selective detection of spores are crucial. In this study, a fluorescent probe was developed based on lanthanide ion (Eu^{3+})-labeled nano-silver-modified graphene oxide (GO-AgNPs-Eu^{3+}) for the detection of 2,6-dipicolinic acid (DPA), a biomarker unique to spores, to allow quantitative spores detection. The GO-AgNPs-Eu^{3+} nano-fluorescent probe was loaded onto a polyvinylidene fluoride microfiltration membrane, and a smartphone-assisted portable GO-AgNPs-Eu^{3+} nanoparticles-based paper visual sensor was designed for rapid on-site quantitative and real-time online detection of spores. The results indicated that the developed probe achieved equilibrium binding with DPA within 5 min, and enhanced fluorescence emission through antenna effect. The fluorescence detection presented a good linear relationship in the DPA concentration range of 0–45 μM, with a DPA detection limit of 4.62 nM and spore detection limit of 10^4 cfu/mL. The developed sensor showed a change in fluorescence from blue to red with increasing DPA concentration, and this color change was quantitatively detected through smartphone RGB variations, with a detection limit of 13.1 μM for DPA and 6.3 cfu/mL for *Bacillus subtilis* spores. Subsequently, the sensitivity and selectivity of the developed sensor were verified using actual milk and water samples spiked with *B. subtilis* spores. The results of this study provided objective technological support for rapid detection of spores, which is important for reducing the occurrence of foodborne diseases and improving food safety.

1. Introduction

Spore is a kind of dormancy body with strong resistance and are primarily composed of DNA, various receptor proteins, peptidoglycan, and pyridine dicarboxylic acid (2,6-dipicolinic acid, DPA) (Farag, Mesak, Saied, & Ezzelarab, 2021; Nakaya et al., 2023; Pande, Perez Escriva, Yu, Sauer, & Velicer, 2020). These spores can survive for several years in a dormant state, and can germinate into metabolically active vegetative cells under suitable growth conditions, producing toxins that can cause food spoilage, deterioration, and even foodborne diseases (Z. Zhu, Bassey, Huang, Zhang, Ali Khan, & Huang, 2022). However, as foodborne spores are small in size (with a diameter of < 2 μm), possess unique structure, and are unculturable, their precise identification and digital quantification cannot be achieved using conventional culture methods (Wong, Kang, Reyes, Teo, & Kah, 2020). Besides, accurate assessment and prediction of the associated food safety risks are challenging, making foodborne spores as one of the most distinctive life forms in the entire biological realm (Y. Zhu et al., 2022). DPA is a unique compound present in the spore core, functioning as a biomarker for spore identification (Gao, Zhang, Huang, Xiang, Wu, & Mao, 2018). To assess the risk of spore contamination in a timely manner, various techniques with high sensitivity have been developed (Liang et al., 2023). Optical fluorescence detection technique offers advantages such as low cost, minimal instrument requirements, portability, and real-time capabilities, making it a more economically competitive option (Su et al., 2021; Tiposoth et al., 2015). Among the reported fluorescence probes used for detecting spore DPA, lanthanide ions (Eu^{3+}) exhibit strong specific chelating affinity with the spore biomarker DPA and emit

* Corresponding author at: College of Food Science and Technology, Henan Agricultural University, Zhengzhou 450002, PR China.
E-mail address: zhu_yaodi@163.com (Y. Zhu).

https://doi.org/10.1016/j.fochx.2023.101069
Received 2 November 2023; Received in revised form 9 December 2023; Accepted 12 December 2023
Available online 14 December 2023

fluorescence at unique wavelengths through absorption energy transfer, enabling rapid DPA detection (Jia et al., 2021). Lanthanide fluorescent probes have long fluorescence lifetimes and narrow emission bands, which effectively eliminate interference from background signals and enhance the accuracy of fluorescence detection (Xu et al., 2018).

Furthermore, silver nanoparticles (AgNPs) are widely studied nanomaterials, which have strong surface plasmon resonance bands in the visible region, making them the best probe for sensitive detection of molecules (Philip & Kumar, 2022). When compared with graphene, graphene oxide (GO), a product of graphite oxidation, contains more active functional groups owing to the introduction of oxygen functional groups (such as -C—O, -C═O, carboxyl groups) during the oxidation process (Dissanayake, Cifuentes, & Humphrey, 2018). GO can react with Ag ions through electrostatic or charge transfer interactions, and the reduced Ag ions form stable GO-Ag nanocomposites on the surface of GO, which can enhance fluorescence signals (Kumari et al., 2020; K. Yuan, Chen, & Chen, 2014). When combined with Eu^{3+}, GO-Ag nanocomposites allow for highly selective and rapid detection of foodborne spores, especially DPA, thus offering a new technological approach for quantitative detection of spores.

In the present study, a novel fluorescent probe, GO-AgNPs-Eu^{3+} nanomaterial, was constructed by using the characteristics of lanthanides and GO-AgNPs for DPA detection, and a visual paper sensor based on GO-AgNPs-Eu^{3+} nanomaterials was developed by combining polyvinylidene fluoride (PVDF) microporous filter with smartphone, which was used for rapid visual detection of spore DPA to realize on-site rapid, quantitative, and real-time online analysis of spores. As shown in Fig. 1, the GO-AgNPs nanoparticles were first prepared, and GO-AgNPs-Eu^{3+} nanomaterials were synthesized and characterized by cross-linking reaction with EDTA via aminochemical treatment. Then, the biomarker DPA of four representative spores (*Clostridium sporogenes* spores, *Bacillus subtilis* spores, *Bacillus cereus* spores, and *Bacillus thuringiensis* spores) was detected using our developed fluorescent probe, and the limit of detection (LOD) of GO-AgNPs-Eu^{3+} nanomaterials for DPA and spores were calculated. Subsequently, a PVDF microporous membrane sensor based on GO-AgNPs-Eu^{3+} nanomaterial was developed and integrated with a smartphone for on-site visual detection of spore DPA. Lastly, the sensitivity and specificity of the developed sensor were validated using actual milk and water samples spiked with *B. subtilis* spores.

2. Methods

2.1. Materials and reagents

The strains *B. thuringiensis*, *B. cereus*, *B. subtilis*, and *C. sporogenes* were obtained from China Culture Preservation Center and Guangdong Huankai Microbial Technology Co., Ltd., China, and stored at −80℃ in a porcelain bead culture preservation. Culture media, including Robertson's cooked meat medium (RCM), Luria–Bertani (LB) medium, Difco sporulation medium (DSM), tryptose sulfite cycloserine (TSC) medium, and nutrient agar (NA) medium, were purchased from Beijing Luqiao Co., Ltd., China. Graphite sheets, sodium nitrate ($NaNO_3$), silver nitrate ($AgNO_3$), potassium permanganate ($KMnO_4$), hydrogen peroxide (H_2O_2), sodium borohydride ($NaBH_4$), 1,2-bis(2-aminoethoxy)ethane, europium nitrate ($Eu(NO_3)_3{\cdot}6H_2O$), ethylenediaminetetraacetic acid dianhydride (EDTAD), and ascorbic acid ($C_6H_8O_6$) were obtained from China National Pharmaceutical Group Chemical Reagent Co., Ltd., China. The glassware used in the experiments was cleaned with aqua regia ($HCl:HNO_3 = 3:1$), rinsed with deionized water, and dried before use.

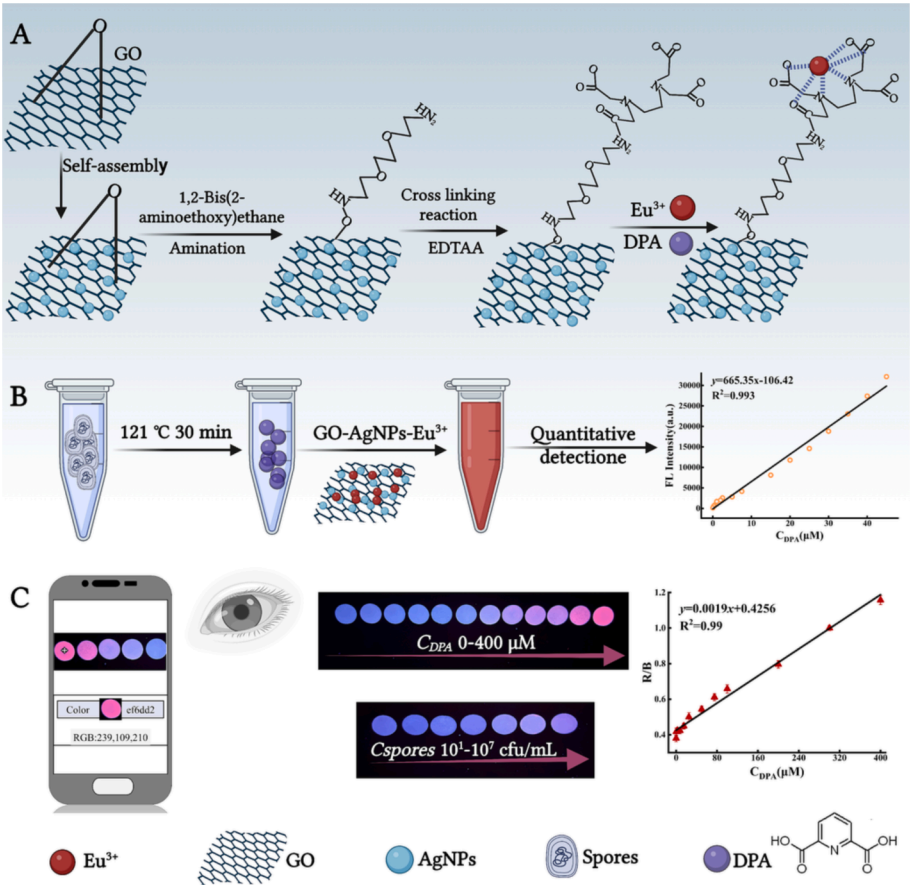

Fig. 1. Preparation of GO-AgNPs-Eu^{3+} nanomaterials and its application in foodborne spores detection.

2.2. Spore cultivation method

Preparation of *C. sporogenes* spores (Y. Zhu et al., 2022; Y. Zhu et al., 2023): *C. sporogenes* spores porcelain beads were streaked onto NA medium to obtain single bacterial colonies, and a single colony was transferred to 20 mL of RCM and incubated for 6 h. Then, 200 μL of the bacterial suspension were inoculated onto RCM solid medium and incubated for 3–7 days. The spores were collected by centrifugation (8,000 rpm, 10 min, 4 °C) and washed with cold sterile deionized water for 5–7 times to remove impurities such as vegetative cells from the spore suspension. After washing, the spores were examined under a microscope, and considered suitable for further analysis when ≥ 95 % of the field of view consisted of translucent spores with no visible small impurities.

Preparation of *B. subtilis* spores: *B. subtilis* spores porcelain beads were streaked onto LB plate and incubated overnight to obtain single bacterial colonies. After three generations of activation, fresh single colonies were selected and transferred to 20 mL of LB medium and incubated overnight (200 rpm, 37℃) until an optical density (OD_{600}) of 1.2–1.5 was reached, and then inoculated into the spore growth promoting medium, DSM, at a ratio of 1:100 (200 rpm, 37℃). Subsequently, the spores were collected as described earlier.

Preparation of *B. cereus* spores: *B. cereus* spores porcelain beads were streaked onto NA plate and cultured overnight until the growth of single bacterial colonies. Then, a single colony was inoculated into 20 mL of nutrient broth and incubated for 6 h at 200 rpm and 37℃, and transferred to NA plate containing 10.05 g/L manganese sulfate tetrahydrate at a ratio of 1:100 and incubated for 2–7 days. Subsequently, the spores were collected as described earlier.

Preparation of *B. thuringiensis* spores: *B. thuringiensis* spores porcelain beads were streaked onto LB plate and cultured overnight until the growth of a single colony. Subsequently, a single colony was inoculated into 20 mL of LB broth and cultured overnight until OD_{600} of 1.2–1.5. Then, 200 μL of the bacterial culture were inoculated onto Insecticidal Crystal Proteins Medium (ICPM) solid medium and incubated for 3–7 days. The spores obtained were collected as previously described.

2.3. Preparation of GO-AgNPs-Eu^{3+} nanomaterials

Synthesis of GO-AgNPs nanomaterials: A total of 0.5 g of graphite sheets and 0.25 g of $NaNO_3$ were mixed with concentrated sulfuric acid, and the mixture was cooled to 0 °C, followed by the addition of $KMnO_4$. After stirring at room temperature for 30 min, ultrapure water and 30 % H_2O_2 were added at 98 °C for 15 min. Subsequently, the mixture was washed sequentially with 0.1 M HCl and water, and vacuum-dried at 60 °C for 12 h to obtain GO (H. Li et al., 2020; Y. Li et al., 2021). Then, 200 μL of 0.5 mg/mL GO were mixed with 19 mL of ultrapure water and continuously stirred for 15 min (pH = 9), and 0.3 mL of $AgNO_3$ (10 mM) was added to the mixture and again continuously stirred for 30 min. Subsequently, 50 μL of 0.01 M $NaBH_4$ were slowly added to the mixture (Loganathan, Muthukrishnan, & John, 2021). After that, 25 mL of 1,2-bis(2-aminoethoxy)ethane, 500 mg of potassium hydroxide, and 250 mL of water were added to the mixture and vigorously stirred for 24 h at 70 °C, and then 50 mL of 0.5 M $NaBH_4$ solution were added to the mixture and incubated at 70 °C for 2 h. The resulting product was collected by centrifugation and thoroughly washed with water several times to obtain the precipitate. Next, 10 mg of the obtained precipitate were dispersed in 5 mL of bicarbonate buffer solution (pH = 9.6, 0.1 M) and mixed with 80 mg of EDTAD by stirring for 2 h. The prepared nanoparticles were separated by centrifugation, washed four times with bicarbonate buffer solution, washed twice with deionized water, and vacuum-dried at 60 °C for 12 h to obtain EDTAD-modified GO-AgNPs nanoparticles (Y. Wang, Li, Qi, & Song, 2015).

Synthesis of GO-AgNPs-Eu^{3+} nanomaterials: A total of 10 mg of GO-AgNPs were dispersed in 5 mL of water and sonicated, followed by dropwise addition of 5 mL of $Eu(NO_3)_3{\cdot}6H_2O$ (0.01 M) with continuous stirring for 3 h. The product obtained was collected by centrifugation, washed several times with deionized water, and resuspended in 5 mL of ultrapure water to obtain a 2 mg/mL solution (M. Yuan et al., 2023).

2.4. Characterization of GO-AgNPs-Eu^{3+} nanomaterials

The UV–Visible spectra of the nanoparticles were assessed using a UV-2600 spectrophotometer (Shimadzu Corporation) with a scanning speed of 0.5 nm/s and wavelength range of 200–800 nm. The morphology and elemental distribution of the nanoparticles were characterized using a scanning electron microscope (SEM, ZEISS Sigma 300) equipped with an energy-dispersive X-ray spectrometer (EDS, Oxford Xplore). The crystal structure and purity of the nanoparticles were determined by X-ray diffraction (XRD) using a TD-3500 X-ray diffractometer with scanning angles ranging from 5° to 80° and scanning speed of 0.1°/s. Elemental composition and oxidation states were analyzed by X-ray photoelectron spectroscopy (XPS) using a Thermo Scientific K-Alpha instrument. Fluorescence spectra were measured using a fluorescence spectrophotometer (F-4600, Hitachi, Japan).

2.5. Fluorescence measurement

A total of 200 μL of samples and 2 μL of GO-AgNPs-Eu^{3+} nanomaterials were added into 500 μL of Tris buffer (10 mM, pH = 7.0), and the emission spectra were collected using a Hitachi F4600 fluorescence spectrophotometer. All the tests were conducted at room temperature, under a scanning rate of 1,200 nm/min, an excitation wavelength of 282 nm, and an emission wavelength of 616 nm. The excitation and emission slits were fixed at 10 nm, and the fluorescence spectrum was scanned at 700 V. The experiment was performed in triplicate (n = 3).

2.6. Detection of spore DPA

The initial concentration of the spores was adjusted to OD_{600} of 0.5 (approximately 10^7 cfu/mL). Then, a certain volume of spore suspension was serially diluted with sterile water, and the diluted spore suspension was inoculated onto corresponding culture medium at 37 °C. After incubation for 24 h, the specific concentration of the spores was determined by plate counting. Subsequently, the spores at different concentrations were heat-treated at 121 °C for 30 min to ensure complete release of DPA. Then, 200 μL of the spore suspension and 2 μL of GO-AgNPs-Eu^{3+} nanomaterials were added to 500 μL of Tris buffer (10 mM, pH = 7.0) and incubated at room temperature for 5 min, and the fluorescence intensity was measured.

2.7. Preparation of GO-AgNPs-Eu^{3+} nanomaterials based visual paper sensor

The PVDF microporous membrane was immersed into Tris buffer (10 mM, pH = 7.0) containing GO-AgNPs-Eu^{3+} nanomaterials (approximately 5 mg/mL) for 20 min and air-dried naturally to develop an instant visual paper sensor for DPA detection. Subsequently, 20 μL of samples at different concentrations were added onto the prepared GO-AgNPs-Eu^3 nanomaterials based visual paper sensor for DPA detection. The fluorescence color change images were captured using a smartphone, and the changes in the red, green, and blue (RGB) values were calculated. Then, the RGB intensity of the images was generated using an installed color recognition app on the smartphone.

3. Results and discussion

3.1. Characterization of GO-AgNPs-Eu^{3+} nanomaterials

After preparing GO by Hummer's method, the GO-AgNPs nanoparticles were synthesized by $NaBH_4$ reduction method, and amination treatment was employed to make the surface of the nanoparticles amino-

functionalized. Subsequently, GO-AgNPs-Eu^{3+} nanomaterials were prepared by two-step surface functionalization method, and EDTA-modified GO-AgNPs nanoparticles were obtained by introducing EDTAD into GO-AgNPs nanoparticles, which caused a spontaneous cross-linking reaction between the anhydride and $–NH_2$, resulting in GO-AgNPs-EDTA. The EDTA ligands on the GO-AgNPs nanoparticles readily formed GO-AgNPs-Eu^{3+} nanomaterials through strong chelation with the Eu^{3+} ions. As shown in Fig. 2A, GO exhibited a broad plasmon resonance peak at around 300 nm. However, during $NaBH_4$ reduction to synthesize GO-AgNPs nanoparticles, the oxygen functional groups of GO were masked, resulting in the disappearance of the absorption peak. Instead, a characteristic absorption peak induced by AgNPs was observed at 390 nm, and the color of the mixture turned yellow. After the binding of EDTA ligand onto GO-AgNPs nanoparticles with Eu^{3+}, the diameter of the nanoparticles increased, resulting in the widening of the ion resonance absorption peak, which preliminarily determined the formation of GO-AgNPs-Eu^{3+} nanomaterials.

To further confirm the successful synthesis of GO-AgNPs-Eu^{3+} nanomaterials, the structure and surface morphology were characterized using scanning electron microscopy (SEM). As shown in Fig. 2G and 2H, AgNPs were well-dispersed on the graphene surface. Comprehensive characterization of the elemental composition of GO-AgNPs-Eu^{3+} nanomaterials using EDS (Fig. 3I–3L) revealed that the particle-like Ag (red) was distributed on the surface of GO (green) and Eu (blue) was uniformly dispersed on the surface of GO-AgNPs nanoparticles. It can be seen that AgNPs have been reduced on the surface of graphene oxide and $–NH_2$ was formed on the surface by amination treatment, followed by the spontaneous cross-linking reaction between the anhydride and $–NH_2$ after the introduction of EDTA to form –COOH and CO-NH groups, and that the AgNPs are uniformly dispersed, which is due to the EDTA enhanced electrostatic repulsion in the presence of EDTA. It has been reported to prove that EDTA has strong chelating effect with Eu^{3+} and effectively hinders the coordination of H_2O with Eu^{3+}, avoiding the loss of non-radiative energy (Tan, Ma, Chen, Xu, Chen, & Wang, 2014; Y. Wang et al., 2015). Furthermore, XRD characterization of the crystalline structure of GO-AgNPs-Eu^{3+} nanomaterials presented a sharp diffraction peak (2θ) at 10.7° for GO (curve (a) in Fig. 2B), and the diffraction peaks (2θ) at 10.7°, 38.24°, 44.4°, 64.5°, and 77.46° for GO-AgNPs (curve (b) in Fig. 2B) corresponded to (001), (111), (200), (220), and (311) crystal planes of GO and Ag cubic structure, respectively, which are consistent with the powder diffraction file database card (JCPDS 75–1609). Moreover, the diffraction peaks (2θ) characteristic of both GO and AgNPs could be noted in curve (b). Characterization of the GO-AgNPs-Eu^{3+} nanomaterials using XPS revealed a deconvoluted XPS C1s region presenting three prominent peaks at 284.1, 285.8, and 287.8 eV, corresponding to sp2 carbon, O—C—O, and O-C═O bonds, respectively (Fig. 2C–2F). Deconvolution of the Ag3d XPS spectrum showed two peaks at binding energies of 367.8 and 373.8 eV for Ag3d5/2 and Ag3d3/2, respectively, indicating the presence of metallic silver (Ag0) in the GO-AgNPs-Eu^{3+} nanomaterials. In addition, two peaks at 1134.1 and 1163.7 eV corresponded to Eu(II) 3d5/2 and Eu(III) 3d5/2, respectively (S. Li, Li, Cao, Zhu, Fan, & Li, 2014; Miao et al., 2023). These characterizations provided strong evidence for the successful synthesis of GO-AgNPs-Eu^{3+} nanomaterials.

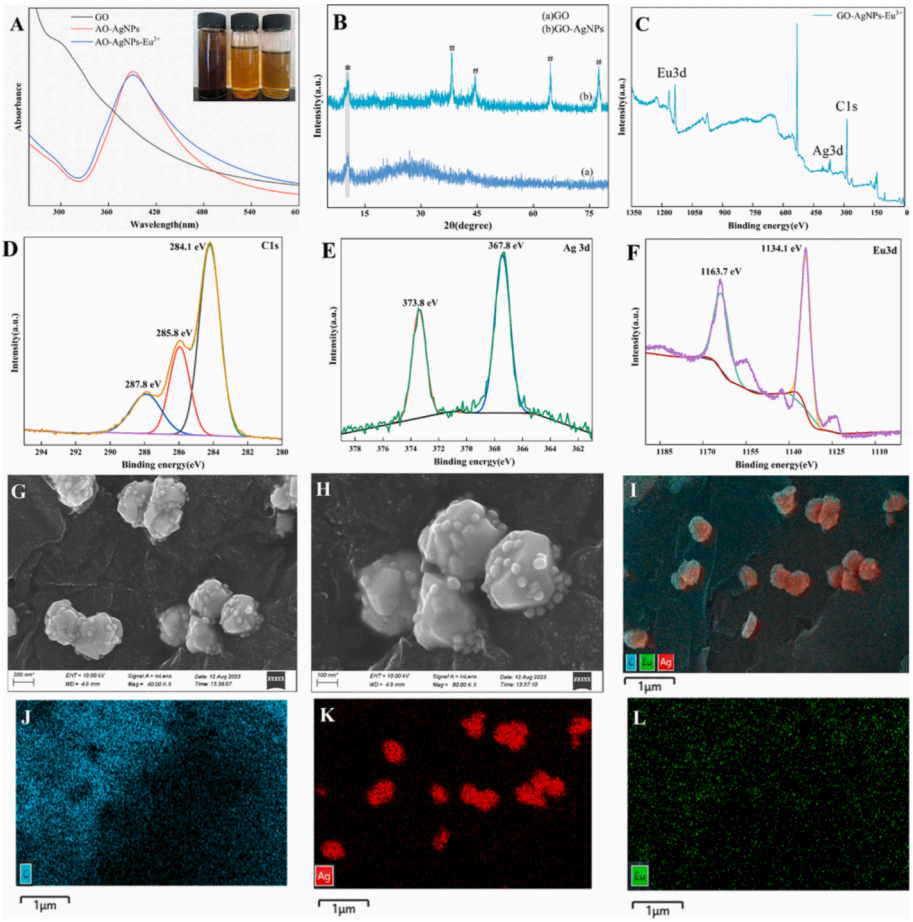

Fig. 2. Characterization of GO-AgNPs-Eu^{3+} nanomaterials. (A) UV–Visible spectrum; (B) XRD characterization of GO-AgNPs-Eu^{3+} nanomaterials; (C) full-scan XPS of GO-AgNPs-Eu^{3+} nanomaterials; (D) XPS spectrum of C1s; (E) XPS spectrum of Ag3d; (F) XPS spectrum of Eu3d; (G and H) SEM images of GO-AgNPs-Eu^{3+} nanomaterials; (I, J, K, and L) EDS elemental mapping of GO-AgNPs-Eu^{3+} nanomaterials.

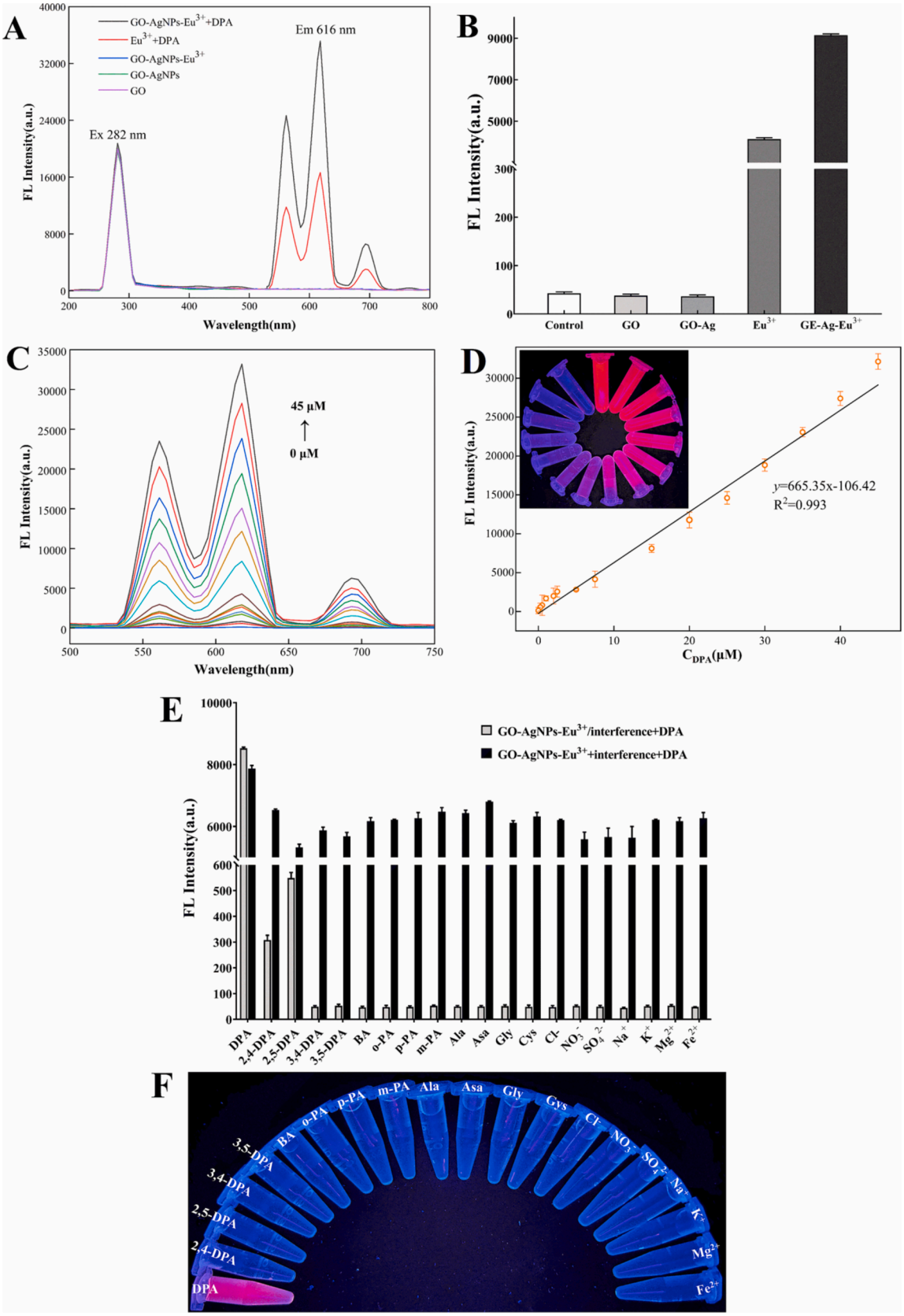

Fig. 3. (A) Fluorescence spectrum of GO-AgNPs-Eu^{3+} nanomaterials; (B) comparison of fluorescence intensity of GO-AgNPs-Eu^{3+} nanomaterials at 616 nm; (C) fluorescence spectra of GO-AgNPs-Eu^{3+} nanomaterials following addition of different concentrations of DPA (0, 0.25, 0.5, 1.0, 2.0, 5.0, 7.5, 15.0, 20.0, 25.0, 30.0, 35.0, 40.0, and 45.0 μM); (D) standard curve of fluorescence intensity of GO-AgNPs-Eu^{3+} nanomaterials vs. DPA concentration; (E) selectivity for DPA and interference resistance of GO-AgNPs-Eu^{3+} nanomaterials (gray bars represent interference solutions in GO-AgNPs-Eu^{3+} nanomaterials, black bars denote subsequent addition of 30 μL of DPA); (F) colored fluorescence photographs of DPA and various interfering substances under 254-nm UV illumination.

3.2. Detection of DPA by GO-AgNPs-Eu^{3+} nanomaterials

EDTA can effectively prevent the access of –OH groups and water, thereby promoting the intrinsic emission of Eu^{3+}. Owing to the specificity and strong chelation affinity between Eu^{3+} and DPA, GO-AgNPs-Eu^{3+} nanomaterials can serve as highly sensitive nanoprobes for detecting DPA (Yang, Lu, Zhan, Tian, Yuan, & Lu, 2020). As shown in Fig. 3A, GO, GO-AgNPs, and GO-AgNPs-Eu^{3+} did not emit the characteristic fluorescence (red fluorescence) of Eu^{3+} at 616 nm. There are two possibilities that the fluorescence of GO-AgNPs-Eu^{3+} is suppressed by the inner filter effect (IFE) or the GO-AgNPs-Eu^{3+} system cannot emit the fluorescence itself (Yin & Tong, 2021). However, after the addition of DPA, a non-fluorescent compound, to the system, the characteristic fluorescence of Eu^{3+} at 616 nm was detected, because the coordination interaction of conjugated organic ligands and energy transfer effects (antenna effect, AE) led to the luminescence of Eu^{3+}(Yin et al., 2021). DPA possesses a pyridine N and two carboxyl groups, which can interact with Eu^{3+} through metal–ligand chelation coordination. When an appropriate surface ligand (DPA) is introduced, the ligand (DPA) acts as an antenna absorbing group, stably chelating with Eu^{3+}, effectively enhancing the red fluorescence of Eu^{3+} through the AE, and transferring energy to Eu^{3+}. Comparison of the fluorescence intensity at 616 nm (Fig. 3B) evidently showed that the fluorescence intensity of GO-AgNPs-Eu^{3+} nanomaterials was significantly higher than that of Eu^{3+}, suggesting that GO-AgNPs nanoparticles play a role in enhancing fluorescence. It must be noted that individual coordination of Eu^{3+} with DPA did not reach saturation, and hence, the Eu^{3+} ions coordinated with water molecules to achieve saturation, resulting in some non-radiative energy loss. In contrast, GO-AgNPs nanoparticles modified with EDTA hindered the coordination of Eu^{3+} with water molecules and, instead, facilitated coordination with the functional groups on the surface of GO-AgNPs nanoparticles, thus preventing energy loss and enhancing fluorescence intensity. Additionally, during the addition of DPA to the GO-AgNPs-Eu^{3+} system, only Eu^{3+} ions that acted as a bridge for connecting the GO-AgNPs are inhibited and the aggregated GO-AgNPs-Eu^{3+} are redispersed. However, the coordination of GO-AgNPs with Eu^{3+} is not destroyed yet, which is the reason why the characteristic fluorescence of Eu^{3+} ions in the GO-AgNPs-Eu^{3+}-DPA system is greatly enhanced compared with that in the Eu^{3+}-DPA system (Yin et al., 2021).

To investigate the sensitivity of GO-AgNPs-Eu^{3+} nanomaterials to DPA, fluorescence emission spectra were observed after the addition of different concentrations of DPA to GO-AgNPs-Eu^{3+} nanomaterials (Fig. 3C). At 0–45 μM DPA concentration, the fluorescence emission peak at 616 nm increased with increasing DPA concentration, exhibiting strongest fluorescence signal. Thus, detection of DPA concentration based on fluorescence intensity at 616 nm could achieve higher sensitivity. As shown in Fig. 3D, the fluorescence intensity of GO-AgNPs-Eu^{3+} nanomaterials presented a strong linear correlation with DPA concentration in the range of 0–45 μM. The linear regression equation was $y = 691.09x - 907.78$, with an R^2 value of 0.99. The LOD of the prepared nanomaterials was calculated using the formula $LOD = 3\sigma/k$, and was found to be 4.62 nM, which was lower than the amount of released DPA (60 μM) that can cause pathogenic spore formation. In addition, comparison of the LOD, detection time, and linear range of the present study with those reported in previous works revealed that the findings of this study were comparable to most of those reported in recent years (Table 1). More importantly, under UV light (254 nm) exposure, a visible color change from colorless to red was observed with increasing DPA concentration, and this obvious color change was exploited in the subsequent application of portable DPA visual sensor.

For practical application, the GO-AgNPs-Eu^{3+} nanomaterials must exhibit selectivity and anti-interference ability; however, some interfering substances may exist during practical applications. Therefore, we examined the ability of our developed nanomaterials to detect different kinds of aromatic ligands, amino acids, and various common cations or anions (3,5-DPA, BA, mPA, p-PA, o-PA, 2,4-DPA, 2,5-DPA, 3,4-DPA, Asa, Ala, Cys, Gly, K^+, Fe^{3+}, Mg^{2+}, Na^+, NO_3^-, Cl^-, SO_4^{2-}) under the same detection conditions (Fig. 3E). The results revealed that only DPA induced a signal response at 616 nm, and none of the interfering substances caused a significant fluorescence change. Besides, under UV light (254 nm) exposure, only DPA emitted distinct red fluorescence, whereas the other interfering substances did not produce noticeable color changes (Fig. 3F). This high selectivity of GO-AgNPs-Eu^{3+} nanomaterials could be attributed to the strong coordination ability of DPA with Eu^{3+} in a tridentate chelation manner.

Table 1
Comparison of the DPA detection performance of our developed GO-AgNPs-Eu^{3+} nanomaterials with that of different lanthanide nanoprobes.

Testing platform	Analytical technique	Detection limit	References
Tb/Eu@bio-MOF	Ratiometric fluorescent	34 nM	(Zhang, Li, Ma, Zhang, & Zheng, 2016)
AgNPs-Tb^{3+}	Fluorescent	6.7 nM	(Tan et al., 2013)
CDs-Tb^{3+}	Fluorescent	0.1 nM	(Liu et al., 2019)
GMP-Tb^{3+}/Eu^{3+}	Ratiometric fluorescence	96 nM	(Donmez, Oktem, & Yilmaz, 2018)
Eu^{3+}-CDs	Ratiometric fluorescence	5 nM	(Shi, Yang, Dong, & Yu, 2018)
hPEI-CD-EDTA-Eu^{3+}	Ratiometric fluorescence	0.19 nM	(Yang et al., 2020)
Eu-GNPs	Fluorescent	1000 nM	(Donmez, Yilmaz, & Kilbas, 2017)
Tb^{3+}/DPA@SiO_2-Eu/GMP	Ratiometric fluorescence	7.3 nM	(Zhou et al., 2017)
GO-AgNPs-Eu^{3+}	Fluorescent	4.62 nM	This study

Furthermore, to investigate the interference resistance of GO-AgNPs-Eu^{3+} nanomaterials to these potential interfering substances, 30 μM DPA was mixed with 200 μM of different interfering substances, respectively, and their signal responses at 616 nm were comparable to that of DPA. This result indicated that GO-AgNPs-Eu^{3+} nanomaterials exhibited strong interference resistance in DPA detection. To demonstrate the stability of GO-AgNPs-Eu^{3+} nanomaterials, the fluorescence intensity of 20 μM DPA was measured 20 times (Fig. S1), and the results produced an *RSD* of 1.36 %, indicating that our developed GO-AgNPs-Eu^{3+} nanomaterials have high repeatability and could have potential use for practical DPA detection in complex environments.

3.3. Validation of GO-AgNPs-Eu^{3+} nanoparticle-based paper visual sensor for quantitative detection of DPA in spores

To further evaluate the performance of the designed GO-AgNPs-Eu^{3+} nanoparticles based visual sensor for the detection of spores, we used our developed sensor to detect the amount of DPA in four common foodborne spores (*C. sporogenes* spores, *B. subtilis* spores, *B. cereus* spores, and *B. thuringiensis* spores). Before fluorescence detection, the spores were diluted to different concentrations, enumerated by plate counting method, and heat-treated at 121℃ for 30 min to ensure complete release of DPA. Fig. 4 shows the fluorescence detection results for the four foodborne spores. Following the addition of different concentrations of spore suspensions, the characteristic fluorescence emission intensity of GO-AgNPs-Eu^{3+} nanomaterials increased with the increasing spore concentration (Fig. 4A). A linear relationship was observed between *C. sporogenes* spores concentration within the range of 3.18×10^1–3.18×10^7 cfu/mL and fluorescence intensity (Fig. 4B). In particular, *C. sporogenes* spores exhibited good linearity between 10^4 and 10^7 cfu/mL, with a linear equation of $y = 2.93 \times 10^{-4}x + 96.56$ ($R^2 = 0.997$), and the LOD for *C. sporogenes* spores was 2.37×10^4 cfu/mL. Similarly, linear relationships were also noted between the concentrations of *B. subtilis* spores (2.54×10^1–2.54×10^7 cfu/mL), *B. cereus* spores (2.63×10^1–2.63×10^7 cfu/mL), and *B. thuringiensis* spores (4.27×10^1–4.27×10^7 cfu/mL) and their corresponding fluorescence intensities, exhibiting good linearity between 10^4 and 10^7 cfu/mL, with linear equations of $y =$

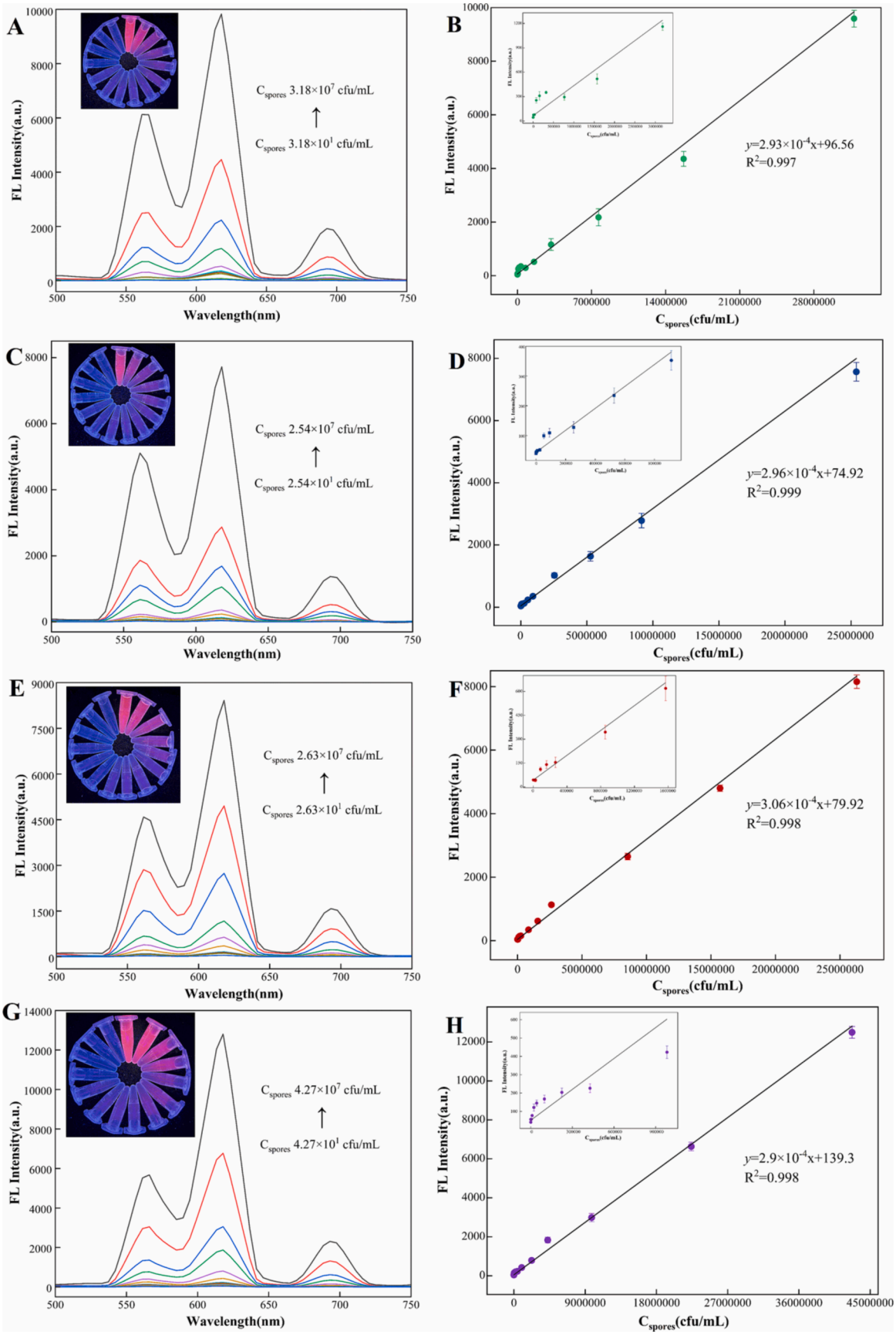

Fig. 4. Fluorescence spectra for different concentrations of (A) *C. sporogenes* spores, (C) *B. subtilis* spores, (E) *B. cereus* spores, and (G) *B. thuringiensis* spores. Fluorescence standard curves for different concentrations of (B) *C. sporogenes* spores, (D) *B. subtilis* spores, (F) *B. cereus* spores, and (H) *B. thuringiensis* spores.

$2.96 \times 10^{-4}x + 74.92$ ($R^2 = 0.999$), $y = 3.06 \times 10^{-4}x + 79.92$ ($R^2 = 0.998$), and $y = 2.9 \times 10^{-4}x + 139.3$ ($R^2 = 0.998$), respectively. The LOD values for *B. subtilis* spores, *B. cereus* spores, and *B. thuringiensis* spores were 2.6×10^4, 2.52×10^4, and 2.66×10^4 cfu/mL, respectively. Furthermore, under UV irradiation (254 nm), gradual visible color change from weak blue to red fluorescence was noted with the increase in spore concentration, and this characteristic red fluorescence of Eu^{3+} at 616 nm could be effectively distinguished without interference. These results suggested that our developed sensor could be directly used to determine the actual spore content, with minimal interference from other components within the spores. Thus, the GO-AgNPs-Eu^{3+} nanomaterials prepared in the present study exhibited high visual detection selectivity for DPA, providing a foundation for the potential application of portable visual sensors for on-site spore detection.

3.4. Validation and application of GO-AgNPs-Eu^{3+} nanoparticles based visual paper sensor

In recent years, there has been a rapid development of instant visual detection technology owing to its advantages of low cost, practicality, and portability (Q. X. Wang et al., 2017; Zhao et al., 2023). In particular, paper-based instant detection devices, as one of the most commonly used substrates, have gained increasing attention. However, conventional filter paper possesses significant inherent fluorescence and uneven distribution of nanoprobes owing to its large micropores (Zhou et al., 2020). In contrast, PVDF microporous membranes have highly compact and fixed internal structures, resulting in well-arranged small micropores and negligible inherent fluorescence (Huang, Xu, Meng, & Li, 2022; Song et al., 2024; Yue et al., 2024). Therefore, this study employed PVDF microporous membrane as the substrate to develop a portable GO-AgNPs-Eu^{3+} nanomaterials based visual paper sensor that presented advantages of high sensitivity, excellent selectivity, and noticeable color change with DPA concentration. In brief, the PVDF microporous filter membrane was first soaked in GO-AgNPs-Eu^{3+} nanomaterial solution and incubated for 20 min (5 mg/mL) and then dried naturally. Subsequently, 20 μL of different concentrations of DPA solution were added onto the PVDF microporous membrane, and images were captured using a smartphone. Finally, the sample was visually analyzed under a handheld UV lamp at 254 nm. As shown in Fig. 5B, with an increase in DPA concentration, the color of the test paper shifted from blue to purple and then to red, which was clearly observable by the naked eye. However, it is difficult to quantify the DPA content using this visual analysis based on color change. Therefore, to achieve digital quantification, a color recognition app installed on a smartphone was

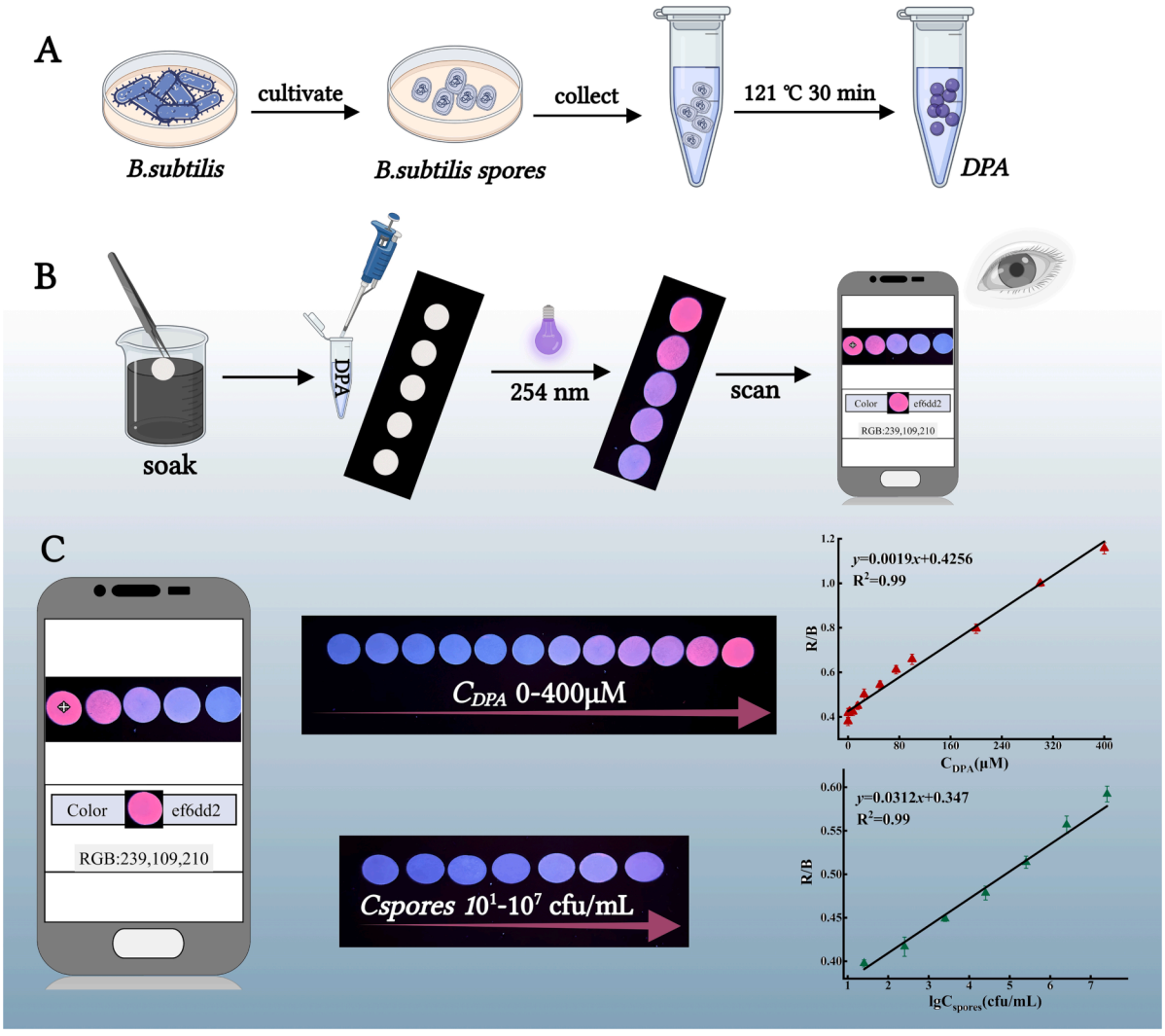

Fig. 5. (A) Process of complete DPA release from *B. subtilis* spores during heat-treatment at 121℃ for 30 min; (B) simplified illustration of DPA detection using the developed GO-AgNPs-Eu^{3+} nanomaterials based visual paper sensor and smartphone sensing platform; (C) fluorescent color image and linear relationship between DPA solution (0–400 μM) and different concentrations of spores solution (10^1–10^7 cfu/mL) under UV irradiation at 254 nm (linear relationship determined between R/B intensity and spores concentration).

used as a signal reader and analyzer, which could digitize the color intensities of RGB in the fluorescence color images and calculate the RGB variation values, allowing for semi-quantitative analysis.

To validate the accuracy of the prepared GO-AgNPs-Eu^{3+} nanomaterials based visual paper sensor for DPA detection, 20 μL of DPA solution (0–400 μM) were added onto the PVDF microporous membrane and allowed to dry. As shown in Fig. 5C, under 254-nm UV light irradiation, the fluorescence color on the PVDF microporous membrane gradually shifted from blue to purple and then to red with increasing DPA concentration, indicating that the designed GO-AgNPs-Eu^{3+} nanomaterials based visual paper sensor successfully achieved visual detection of DPA. Furthermore, the ratio of R to B (R/B) could reflect the concentration of DPA (0–400 μM), which exhibited a good linear relationship with the G/B ratio ($R^2 = 0.99$), and the corresponding linear regression equation was $y(R/B) = 0.00019x\ (CDPA) + 0.4256$, with an LOD of 13.1 μM. These results indicated that smartphone-assisted color analysis based on the GO-AgNPs-Eu^{3+} nanomaterials based visual paper sensor has significant potential use in the field of DPA detection.

Subsequently, the practical application of the GO-AgNPs-Eu^{3+} nanomaterials based visual paper sensor for actual spores detection was confirmed using *B. subtilis* spores. In brief, different concentrations of *B. subtilis* spores (2.54×10^1–2.54×10^7 cfu/mL) were heat-treated at 121 °C for 30 min to ensure complete DPA release (Fig. 5A). Then, the GO-AgNPs-Eu^{3+} nanomaterials based visual paper sensor was used to test the DPA content in different concentrations of spores. As shown in Fig. 5C, with the increasing concentration of *B. subtilis* spores, the fluorescence color on the PVDF microporous membrane gradually shifted from blue to purple under UV light exposure, indicating that the designed paper sensor could visually detect real spores. Furthermore, the logarithmic value of spore concentration presented a good linear relationship with G/B ratio ($R^2 = 0.99$), and the corresponding linear regression equation was $y(R/B) = 0.0312x(\lg C\ spores) + 0.347$, with an LOD of 6.3 cfu/mL. These results demonstrated that the combination of the visual paper sensor with smartphone-assisted color analysis provided technical support for the rapid and convenient detection of real spore samples.

To assess the feasibility of the GO-AgNPs-Eu^{3+} nanomaterials based visual paper sensor for detecting foodborne spores in complex environments, a spiked experiment was designed to measure the spores content in tap water and milk samples using fluorescence detection and a smartphone sensing platform. Before spiking the milk samples with spores, the samples were poured into sterile bags and exposed to UV light on both sides for 30 min to eliminate interference from miscellaneous bacteria. Subsequently, the samples were double-filtered using sterile 0.45-μm microporous membranes to remove residual impurities such as proteins. The tap water samples were filtered twice with 0.45-μM sterile microporous membrane to remove insoluble substances. However, pretreatment of dark-colored samples may require further optimization. After samples pretreatment, 1 mL of *B. subtilis* spores at different concentrations (2.54×10^5, 2.54×10^6, and 2.54×10^7 cfu/mL) was added to 9 mL of the actual samples, and the spiked samples were subjected to DPA detection by fluorescence detection and smartphone sensor platform. The results showed that the recovery rate of *B. subtilis* spores by fluorescence detection was 97.5 %–101.8 %, with *RSD* value of 1.5 %–4.6 % (Tables S2 and S3), while that by the smartphone sensor platform was 96 %–103.3 %, with *RSD* value of 2.5 %–7.2 %, demonstrating good recovery rate and small relative standard deviation (n = 3). These findings revealed that GO-AgNPs-Eu^{3+} nanomaterials based fluorescence and smartphone sensor platform had significant potential use in detecting foodborne spores. Based on the chromatic changes of the strip, enabling inexpensive preparation and good portability. The visible color transition of the DPA obviates the need for sophisticated protocols and instruments and provides simple sensors suitable for on-site testing. In the future, along with improving the detection limit, we believe that this paper strip sensor can be widely used in on-site testing and will play an important role in food safety, water source safety and transportation safety where needed.

4. Conclusion

The strong selectivity and chelating affinity between Eu^{3+} and DPA as well as the intense red fluorescence under UV excitation allowed sensitive, accurate, and rapid fluorescence detection and quantification of the spore biomarker DPA. In the present study, novel GO-AgNPs-Eu^{3+} nanomaterials fluorescent probe was developed by binding Eu^{3+} onto GO-AgNPs for the detection of four common bacterial spores (*C. sporogenes* spores, *B. subtilis* spores, *B. cereus* spores, and *B. thuringiensis* spores). The developed system presented excellent performance, achieving an LOD as low as 4.62 nM for DPA and 10^4 cfu/mL for the four spores. Subsequently, a portable GO-AgNPs-Eu^{3+} nanomaterials loaded PVDF micropore membrane was developed, to create a smartphone-assisted portable GO-AgNPs-Eu^{3+} nanomaterials based visual paper sensor, which could quickly detect DPA and visually exhibit color change from blue to red under 254-nm UV irradiation. The developed visual paper sensor combined with a smartphone could be used for rapid measurements and real-time online analysis of spore DPA, providing technical support for on-site detection of spores.

CRediT authorship contribution statement

Jiaqi Tian: Conceptualization, Resources, Supervision, Writing – review & editing. **Qiancheng Tu:** Data curation, Investigation, Writing – original draft. **Miaoyun Li:** Writing – original draft. **Lijun Zhao:** Supervision. **Yaodi Zhu:** Funding acquisition, Investigation. **Jong-Hoon Lee:** Data curation. **Zhengyan Gai:** Supervision. **Gaiming Zhao:** Investigation. **Yangyang Ma:** Writing – review & editing.

Declaration of competing interest

The authors declare that they have no known competing financial interests or personal relationships that could have appeared to influence the work reported in this paper.

Data availability

Data will be made available on request.

Acknowledgments

This research was supported by the Major science and technology projects in Henan province (221100110500), the Major special science and technology projects in Henan Province (231100110400), the key science and technology projects in Henan Province (232102110136), the joint fund of science and technology research and development plan in Henan Province (applied research) (232103810023), the Science and Technology Innovation Team of Henan Universities (22IRTSTHN021) and the National Modern Agriculture (beef yak) Industrial Technology System Construction Special (CARS-37).

Appendix A. Supplementary data

Supplementary data to this article can be found online at https://doi.org/10.1016/j.fochx.2023.101069.

References

Dissanayake, D. M. A. S., Cifuentes, M. P., & Humphrey, M. G. (2018). Optical limiting properties of (reduced) graphene oxide covalently functionalized by coordination complexes. *Coordination Chemistry Reviews, 375*, 489–513. https://doi.org/10.1016/j.ccr.2018.05.003

Farag, M. A., Mesak, M. A., Saied, D. B., & Ezzelarab, N. M. (2021). Uncovering the dormant food hazards, a review of foodborne microbial spores' detection and inactivation methods with emphasis on their application in the food industry. *Trends*

in Food Science & Technology, 107, 252–267. https://doi.org/10.1016/j.tifs.2020.10.037

Gao, N., Zhang, Y., Huang, P., Xiang, Z., Wu, F. Y., & Mao, L. (2018). Perturbing tandem energy transfer in luminescent heterobinuclear lanthanide coordination polymer nanoparticles enables real-time monitoring of release of the anthrax biomarker from bacterial spores. *Analytical Chemistry, 90*(11), 7004–7011. https://doi.org/10.1021/acs.analchem.8b01365

Huang, T., Xu, Y., Meng, M., & Li, C. (2022). PVDF-based molecularly imprinted ratiometric fluorescent test paper with improved visualization effect for catechol monitoring. *Microchemical Journal, 178*. https://doi.org/10.1016/j.microc.2022.107369

Jia, L., Chen, X., Xu, J., Zhang, L., Guo, S., Bi, N., & Zhu, T. (2021). A smartphone-integrated multicolor fluorescence probe of bacterial spore biomarker: The combination of natural clay material and metal-organic frameworks. *Journal of Hazardous Materials, 402*, Article 123776. https://doi.org/10.1016/j.jhazmat.2020.123776

Kumari, S., Sharma, P., Yadav, S., Kumar, J., Vij, A., Rawat, P., … Majumder, S. (2020). A novel synthesis of the graphene oxide-silver (GO-Ag) nanocomposite for unique physiochemical applications. *ACS Omega, 5*(10), 5041–5047. https://doi.org/10.1021/acsomega.9b03976

Li, H., Huang, X., Mehedi Hassan, M., Zuo, M., Wu, X., Chen, Y., & Chen, Q. (2020). Dual-channel biosensor for Hg2+ sensing in food using Au@Ag/graphene-upconversion nanohybrids as metal-enhanced fluorescence and SERS indicators. *Microchemical Journal, 154*. https://doi.org/10.1016/j.microc.2019.104563

Li, S., Li, Y., Cao, J., Zhu, J., Fan, L., & Li, X. (2014). Sulfur-doped graphene quantum dots as a novel fluorescent probe for highly selective and sensitive detection of Fe(3+). *Analytical Chemistry, 86*(20), 10201–10207. https://doi.org/10.1021/ac503183y

Li, Y., Li, Y., Zhang, D., Tan, W., Shi, J., Li, Z., … Zou, X. (2021). A fluorescence resonance energy transfer probe based on functionalized graphene oxide and upconversion nanoparticles for sensitive and rapid detection of zearalenone. *Lwt, 147*. https://doi.org/10.1016/j.lwt.2021.111541

Liang, D., Cui, X., Li, M., Zhu, Y., Zhao, L., Liu, S., … Xu, L. (2023). Effects of sporulation conditions on the growth, germination, and resistance of Clostridium perfringens spores. *International Journal of Food Microbiology, 396*, Article 110200. https://doi.org/10.1016/j.ijfoodmicro.2023.110200

Loganathan, C., Muthukrishnan, K., & John, S. A. (2021). Colorimetric and "turn-on" fluorescence detection of saccharin using silver nanoparticles-graphene oxide composite. *Sensors and Actuators B: Chemical, 341*. https://doi.org/10.1016/j.snb.2021.129967

Miao, P., Zhou, Y., Li, C., Li, J., Wang, W., Ma, T., … Yan, M. (2023). Near-infrared light-induced photoelectrochemical biosensor based on plasmon-enhanced upconversion nanocomposites for microRNA-155 detection with cascade amplifications. *Biosensors & Bioelectronics, 226*, Article 115145. https://doi.org/10.1016/j.bios.2023.115145

Nakaya, Y., Uchiike, M., Hattori, M., Moriyama, M., Abe, K., Kim, E., … Sato, T. (2023). Identification of CgeA as a glycoprotein that anchors polysaccharides to the spore surface in Bacillus subtilis. *Molecular Microbiology, 120*(3), 384–396. https://doi.org/10.1111/mmi.15126

Pande, S., Perez Escriva, P., Yu, Y. N., Sauer, U., & Velicer, G. J. (2020). Cooperation and cheating among germinating spores. *Current Biology, 30*(23), 4745–4752 e4744. https://doi.org/10.1016/j.cub.2020.08.091

Philip, A., & Kumar, A. R. (2022). The performance enhancement of surface plasmon resonance optical sensors using nanomaterials: A review. *Coordination Chemistry Reviews, 458*. https://doi.org/10.1016/j.ccr.2022.214424

Song, W., Zhai, X., Shi, J., Zou, X., Xue, Y., Sun, Y., … Povey, M. (2024). A ratiometric fluorescence amine sensor based on carbon quantum dot-loaded electrospun polyvinylidene fluoride film for visual monitoring of food freshness. *Food Chemistry, 434*, Article 137423. https://doi.org/10.1016/j.foodchem.2023.137423

Su, P., Liang, L., Wang, T., Zhou, P., Cao, J., Liu, W.-S., & Tang, Y. (2021). AIE-based Tb3+ complex self-assembled nanoprobe for ratiometric fluorescence detection of anthrax spore biomarker in water solution and actual spore samples. *Chemical Engineering Journal, 413*. https://doi.org/10.1016/j.cej.2020.127408

Tan, H., Ma, C., Chen, L., Xu, F., Chen, S., & Wang, L. (2014). Nanoscaled lanthanide/nucleotide coordination polymer for detection of an anthrax biomarker. *Sensors and Actuators B: Chemical, 190*, 621–626. https://doi.org/10.1016/j.snb.2013.09.024

Tiposoth, P., Khamsakhon, S., Ketsub, N., Pongtharangkul, T., Takashima, I., Ojida, A., … Wongkongkatep, J. (2015). Rapid and quantitative fluorescence detection of pathogenic spore-forming bacteria using a xanthene-Zn(II) complex chemosensor. *Sensors and Actuators B: Chemical, 209*, 606–612. https://doi.org/10.1016/j.snb.2014.11.113

Wang, Q. X., Xue, S. F., Chen, Z. H., Ma, S. H., Zhang, S., Shi, G., & Zhang, M. (2017). Dual lanthanide-doped complexes: The development of a time-resolved ratiometric fluorescent probe for anthrax biomarker and a paper-based visual sensor. *Biosensors & Bioelectronics, 94*, 388–393. https://doi.org/10.1016/j.bios.2017.03.027

Wang, Y., Li, Y., Qi, W., & Song, Y. (2015). Luminescent lanthanide graphene for detection of bacterial spores and cysteine. *Chemical Communications (London), 51*(55), 11022–11025. https://doi.org/10.1039/c5cc02889b

Wong, Y. L., Kang, W. C. M., Reyes, M., Teo, J. W. P., & Kah, J. C. Y. (2020). Rapid detection of carbapenemase-producing enterobacteriacae based on surface-enhanced raman spectroscopy with gold nanostars. *ACS Infectious Diseases, 6*(5), 947–953. https://doi.org/10.1021/acsinfecdis.9b00318

Xu, J., Shen, X., Jia, L., Zhang, C., Ma, T., Zhou, T., … Li, Y. (2018). A ratiometric nanosensor based on lanthanide-functionalized attapulgite nanoparticle for rapid and sensitive detection of bacterial spore biomarker. *Dyes and Pigments, 148*, 44–51. https://doi.org/10.1016/j.dyepig.2017.09.006

Yang, H., Lu, F., Zhan, X., Tian, M., Yuan, Z., & Lu, C. (2020). A Eu(3+)-inspired fluorescent carbon nanodot probe for the sensitive visualization of anthrax biomarker by integrating EDTA chelation. *Talanta, 208*, Article 120368. https://doi.org/10.1016/j.talanta.2019.120368

Yin, S., & Tong, C. (2021). Europium(III)-modified silver nanoparticles as ratiometric colorimetric and fluorescent dual-mode probes for selective detection of dipicolinic acid in bacterial spores and lake waters. *ACS Applied Nano Materials, 4*(5), 5469–5477. https://doi.org/10.1021/acsanm.1c00838

Yuan, K., Chen, L., & Chen, Y. (2014). Optical engineering of uniformly decorated graphene oxide nanoflakes via in situ growth of silver nanoparticles with enhanced plasmonic resonance. *ACS Applied Materials & Interfaces, 6*(23), 21069–21077. https://doi.org/10.1021/am505916q

Yuan, M., Jin, Y., Yu, L., Bu, Y., Sun, M., Yuan, C., & Wang, S. (2023). Europium-modified carbon nitride nanosheets for smartphone-based fluorescence sensitive recognition of anthrax biomarker dipicolinic acid. *Food Chemistry, 398*, Article 133884. https://doi.org/10.1016/j.foodchem.2022.133884

Yue, X., Fu, L., Zhou, J., Li, Y., Li, M., Wang, Y., & Bai, Y. (2024). Fluorescent and smartphone imaging detection of tetracycline residues based on luminescent europium ion-functionalized the regular octahedral UiO-66-NH(2). *Food Chemistry, 432*, Article 137213. https://doi.org/10.1016/j.foodchem.2023.137213

Zhao, Y., Liu, M., Zhou, S., Yan, Z., Tian, J., Zhang, Q., & Yao, Z. (2023). Smartphone-assisted ratiometric sensing platform for on-site tetracycline determination based on europium functionalized luminescent Zr-MOF. *Food Chemistry, 425*, Article 136449. https://doi.org/10.1016/j.foodchem.2023.136449

Zhou, C., You, T., Jang, H., Ryu, H., Lee, E. S., Oh, M. H., … Jeon, T. J. (2020). Aptamer-conjugated polydiacetylene colorimetric paper chip for the detection of bacillus thuringiensis spores. *Sensors (Basel), 20*(11). https://doi.org/10.3390/s20113124

Zhu, Y., Liu, W., Liu, S., Li, M., Zhao, L., Xu, L., … Yu, Q. (2022). Preparation of AgNPs self-assembled solid-phase substrate via seed-mediated growth for rapid identification of different bacterial spores based on SERS. *Food Research International, 160*, Article 111426. https://doi.org/10.1016/j.foodres.2022.111426

Zhu, Y., Tian, J., Liu, S., Li, M., Zhao, L., Liu, W., … Tu, Q. (2023). Rapid capture and quantification of food-borne spores based on the double-enhanced Fe(3)O(4)@PEI@Ag@PEI core-shell structure SERS sensor. *Spectrochimica Acta. Part A, Molecular and Biomolecular Spectroscopy, 305*, Article 123512. https://doi.org/10.1016/j.saa.2023.123512

Zhu, Z., Bassey, A. P., Huang, T., Zhang, Y., Ali Khan, I., & Huang, M. (2022). The formation, germination, and cold plasma inactivation of bacterial spore. *Food Chemistry Advances, 1*. https://doi.org/10.1016/j.focha.2022.100056